



# Disentangling the effects of temperature and substrate availability on soil CO<sub>2</sub> efflux



Bhaskar Mitra<sup>1</sup>, Asko Noormets<sup>1</sup>, Guofang Miao<sup>1</sup>,  
Steve G. McNulty<sup>2</sup>, Ge Sun<sup>2</sup>, Michael Gavazzi<sup>2</sup> and John S. King<sup>1</sup>

<sup>1</sup> Department of Forestry and Environmental Resources, North Carolina State University, Raleigh, North Carolina, USA  
<sup>2</sup> Eastern Forest Environmental Threat Assessment Center, USDA Forest Service, Raleigh, North Carolina, USA

## Background

Soil respiration ( $R_s$ ) originates from the decomposition of soil microbes, root and rhizosphere respiration and is modulated by photosynthesis and meteorological forcing at different temporal resolution. Despite the complex interactions, scientific community has struggled to move beyond a simple temperature-based quantification of  $R_s$  and develop a theoretical framework that will incorporate the abiotic (soil moisture ( $\theta$ ) and soil temperature ( $T_{s5}$ )) and biotic (photosynthesis) drivers of soil carbon flux. We addressed these critical issues in two North Carolina coastal plain loblolly pine (*Pinus taeda*) plantations (Figure 1) of different vegetation height (Table 1) as well as hydrologic conditions (Figure 2). Our methodology encompassed wavelet (WT) and cross wavelet transformation (CWT) of continuous 30-minute measurements of  $R_s$ ,  $\theta$ ,  $T_{s5}$  and photosynthetically active radiation (PAR) data. PAR was used as a surrogate of photosynthesis. In an attempt to move beyond temperature in understanding  $R_s$ , the following two interrelated objectives have been addressed:

1. What do  $Q_{10}$  model residuals tell us about the unaccounted processes affecting  $R_s$ ?
2. How does variability caused by different hydrologic regimes and stand age induce the dynamics of the multi-temporal relationship between  $R_s$  and environmental ( $T_{s5}$ ,  $\theta$ ) and biological ( $GPP$ ) drivers?

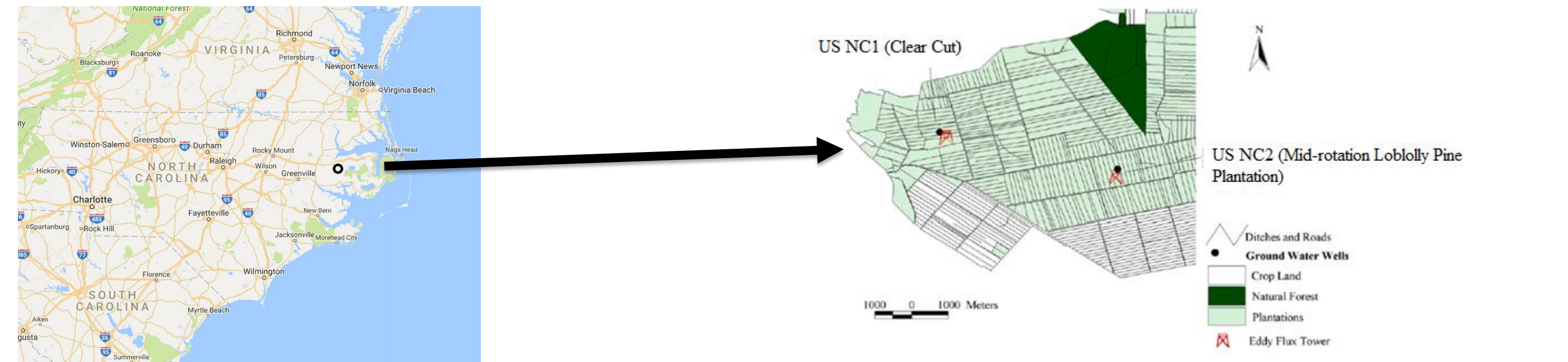


Figure 1: The study site (35°48'N, 76°40'W) was located near the city of Plymouth along the coastal plain forests of North Carolina. The sites are designated as US NC1 and US NC2 in the Ameriflux database.

## Site Description & Measurements

Two stands were selected (Fig. 1; Table 1). The first site was US NC1 (clear cut or early rotation plantation) and has an area of 70 ha. The other site, known as US NC2 (mid rotation plantation) was located less than 3 Km from the CC site and has an area of 100 ha.  $R_s$  and meteorological data for US NC1 and US NC2 have been summarized in Figures 3 and 4 respectively.

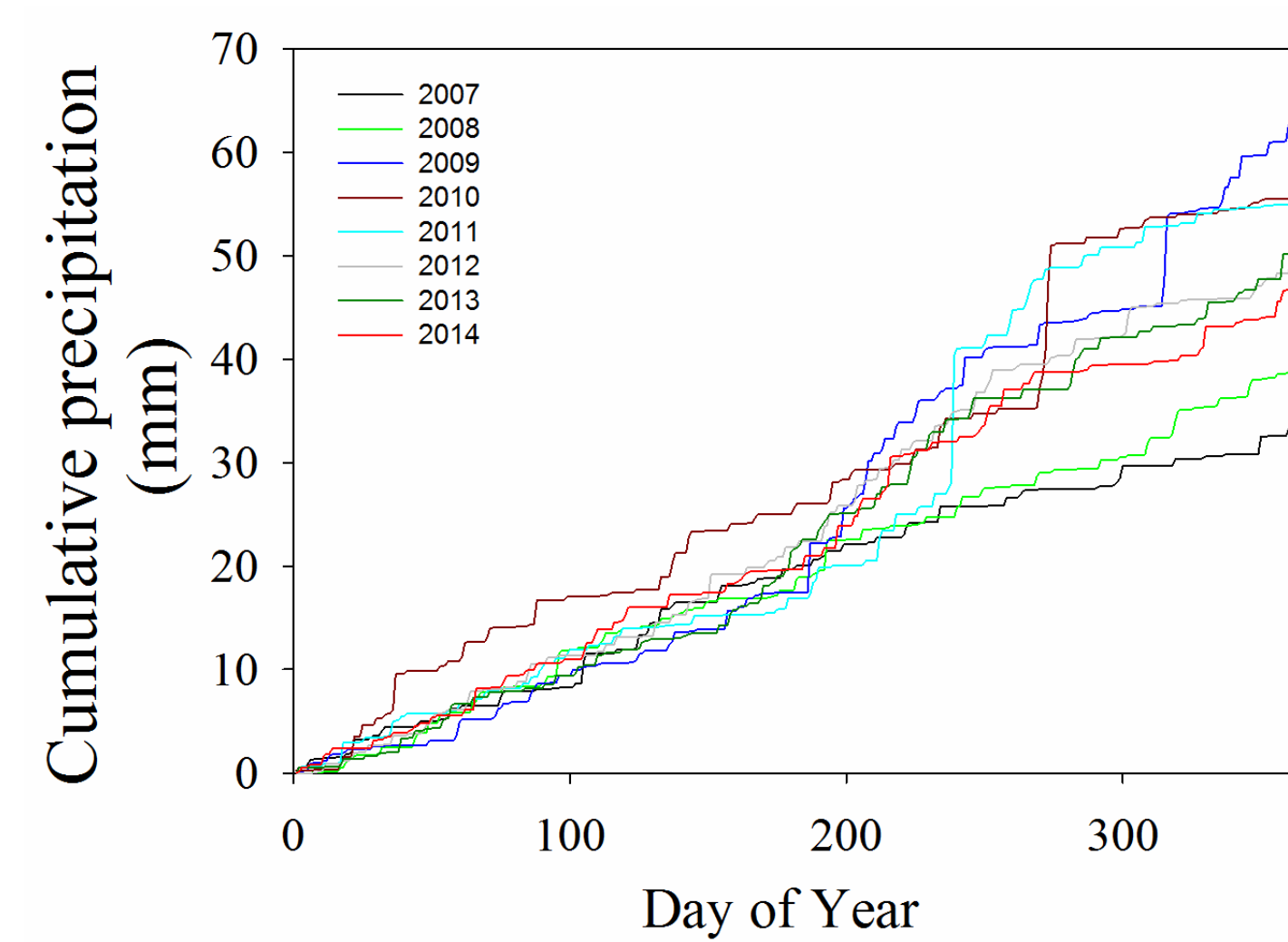


Figure 2: Time series of cumulative precipitation obtained from Plymouth

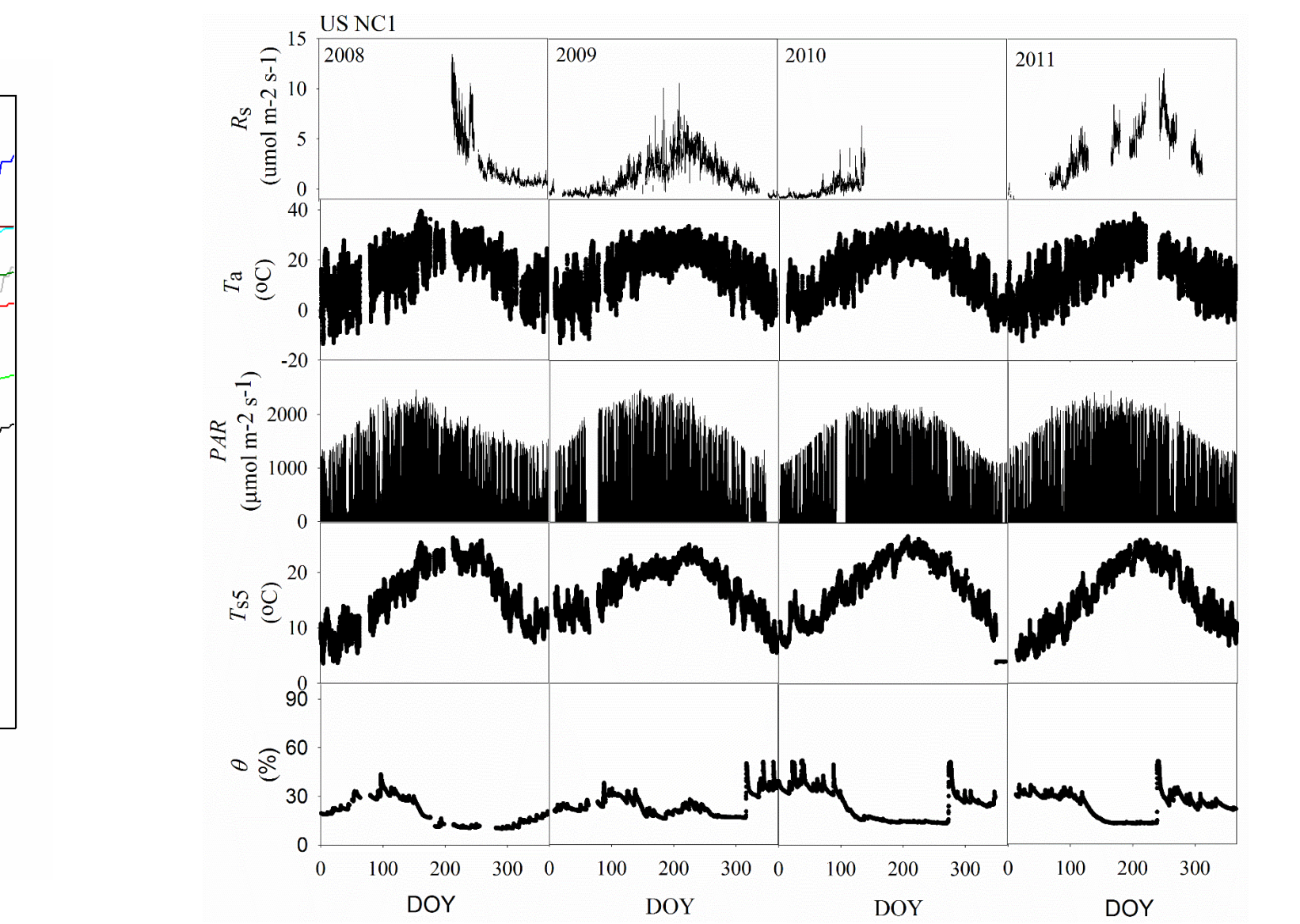


Figure 3: Seasonal variation of 30-minute  $R_s$ , air temperature ( $T_a$ ), PAR,  $T_{s5}$  (5 cm depth),  $\theta$  (30 cm depth) across US-NC1.

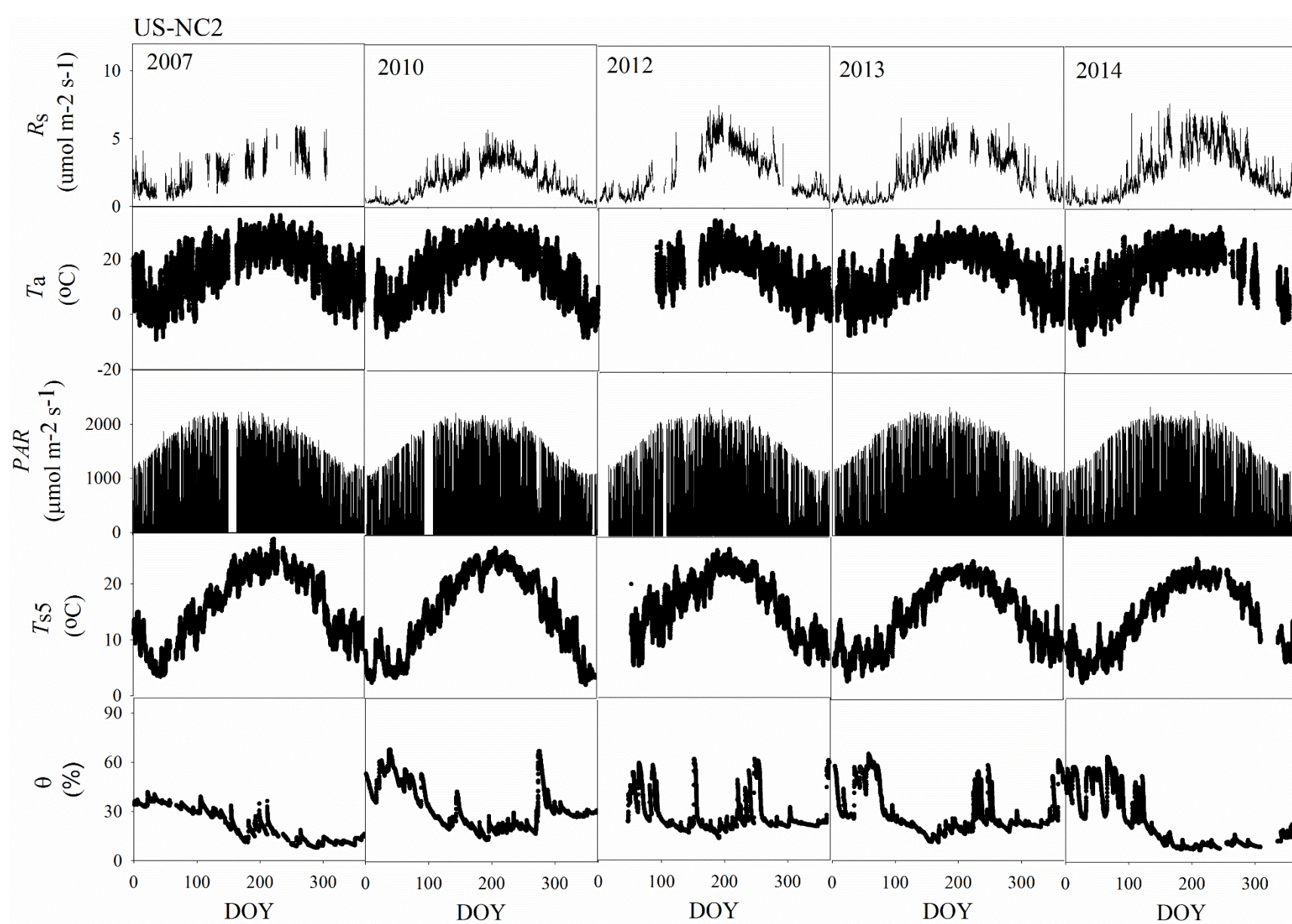


Figure 4: Seasonal variation of 30-minute  $R_s$ , air temperature ( $T_a$ ), PAR,  $T_{s5}$  (5 cm depth),  $\theta$  (30 cm depth) across US-NC2.

Table 1: Summary of average vegetation height for US NC1 and US NC2

Ameriflux Site	Year	Avg. Vegetation Height (m)
US NC1	2008	3
	2009	5
	2010	6.5
	2011	8.5
US NC2	2007	14.1
	2010	17
	2012	19
	2013	20
	2014	21

- **Objective 1:** Moving beyond  $r^2$  - analyzing a simple temperature response function.

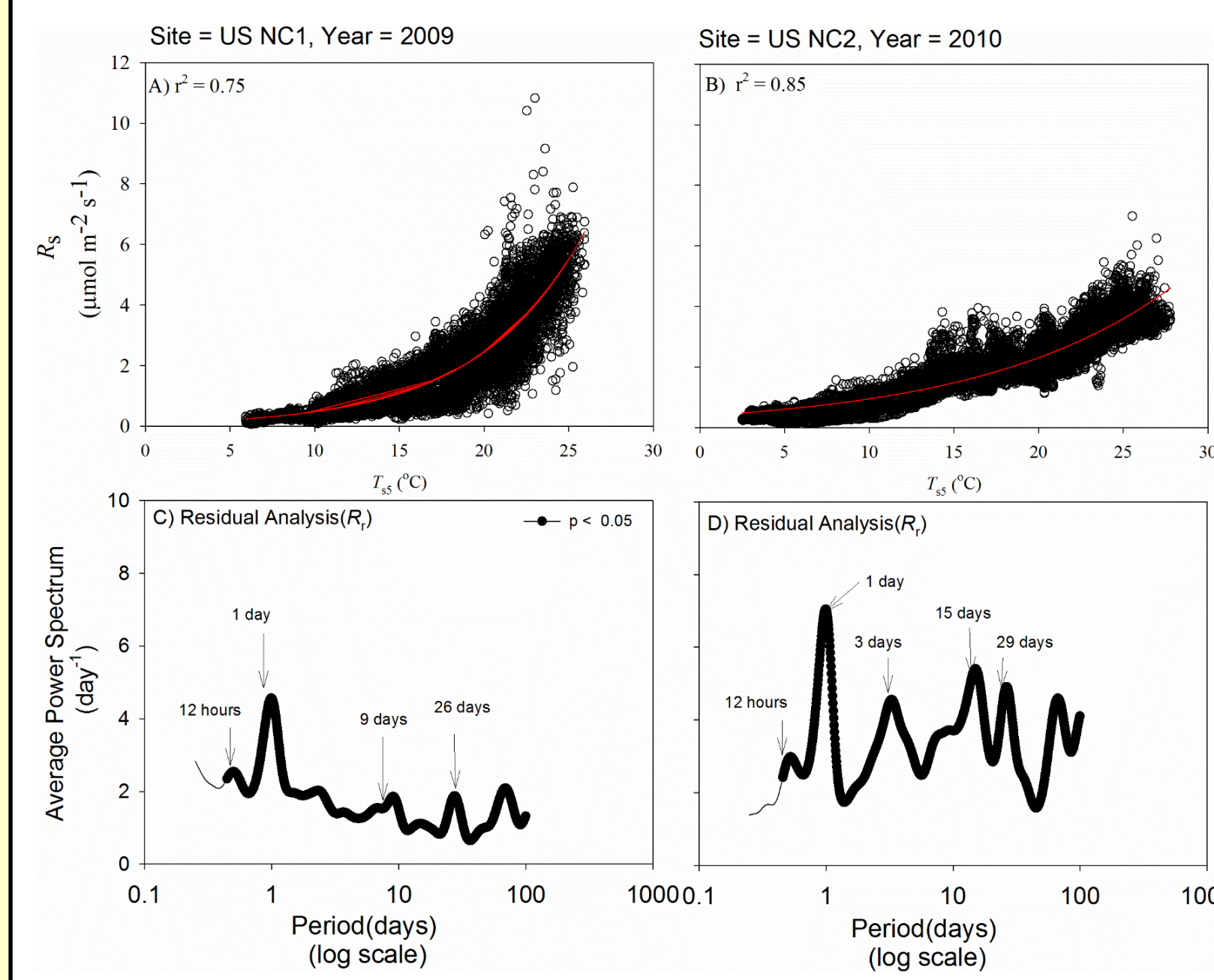


Figure 5: Seasonal variation of soil respiration ( $R_s$ ) against soil temperature ( $T_{s5}$ ). Figures 5C-D highlights the continuous average wavelet power spectra for the residuals ( $R_r$ ) of the corresponding exponential  $Q_{10}$  function fit.

Single temperature exponential  $Q_{10}$  function provided a strong fit to the measured  $R_s$  data at both sites (Figures 5A-B).

However, WT transformation of model residuals ( $R_r$ ) reflected significant variation ( $p < 0.05$ ) in the average global power spectrum at multiple time scales: (Figures 5C-D). The 5% significance level was generated against white noise

Model failure across different periods by the temperature exponential  $Q_{10}$  function was consistent with previous research on ecosystem model analysis (Stoy et al., 2013).

Failure to capture variability in carbon fluxes on the timeframe of weeks and months highlights the lack of proper understanding of biological forcing driving soil carbon flux (Stoy et al., 2005; Dietze et al., 2011).

- **Objective 2:** Multi-temporal relationship between  $R_s$  and biotic and abiotic drivers.
- Figure 6:  $R_s$  and  $\theta$  cospectra exhibited significant ( $p < 0.05$ ) peaks at the synoptic ( $> 7$  days) and monthly ( $> 30$  days) time scale.
- Figure 7:  $R_s$  and  $T_{s5}$  cospectra showed significant peaks at the diurnal, synoptic ( $> 7$  days) and monthly scale.
- Figures 8:  $R_s$  and PAR cospectra exhibited significant ( $p < 0.05$ ) peaks only at the 12-hour and daily frequencies.

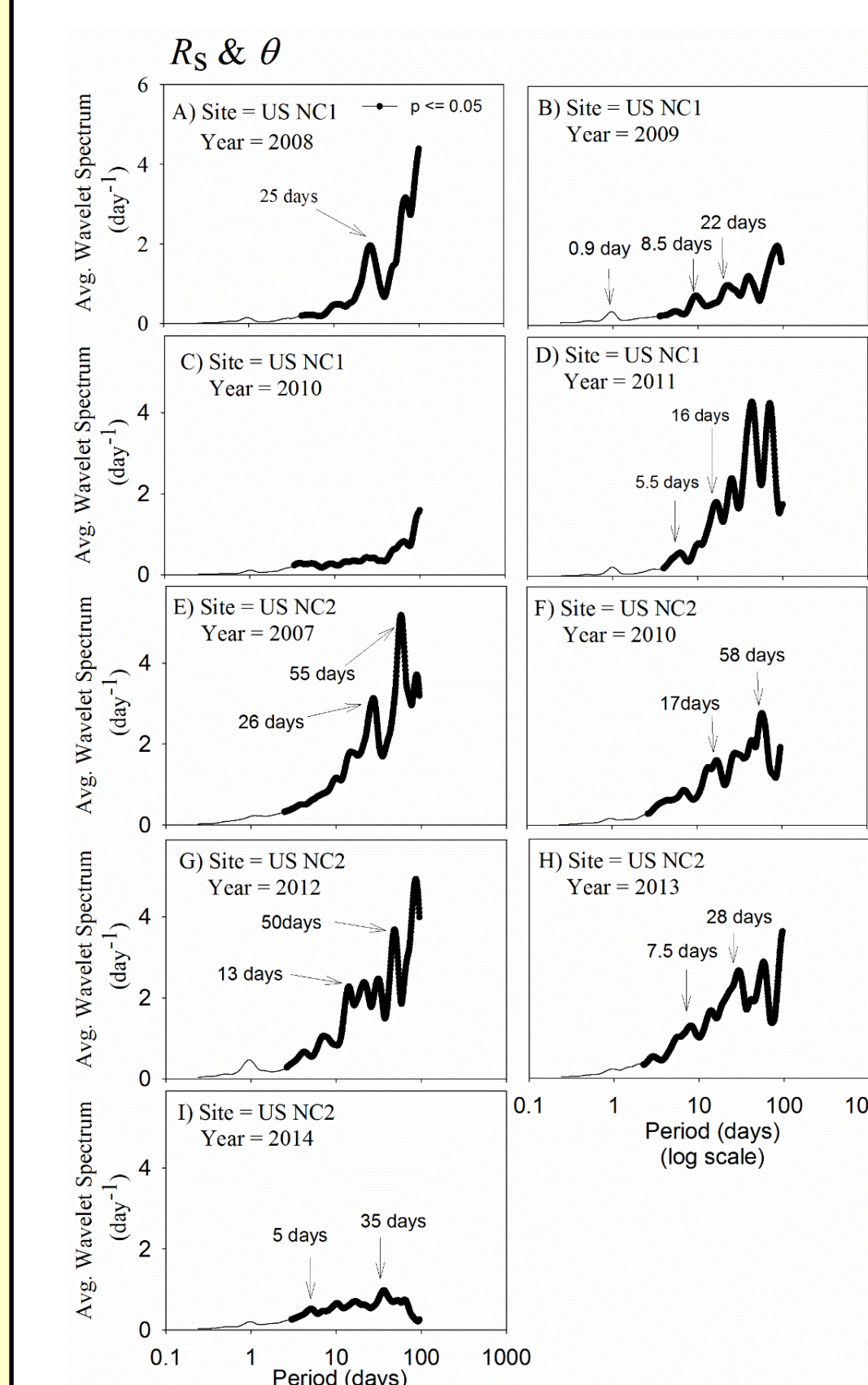


Figure 6: Average wavelet power in the frequency domain generated from CWT transformation of  $R_s$  and  $\theta$  at different sites. The 5% significance level was generated against white noise.

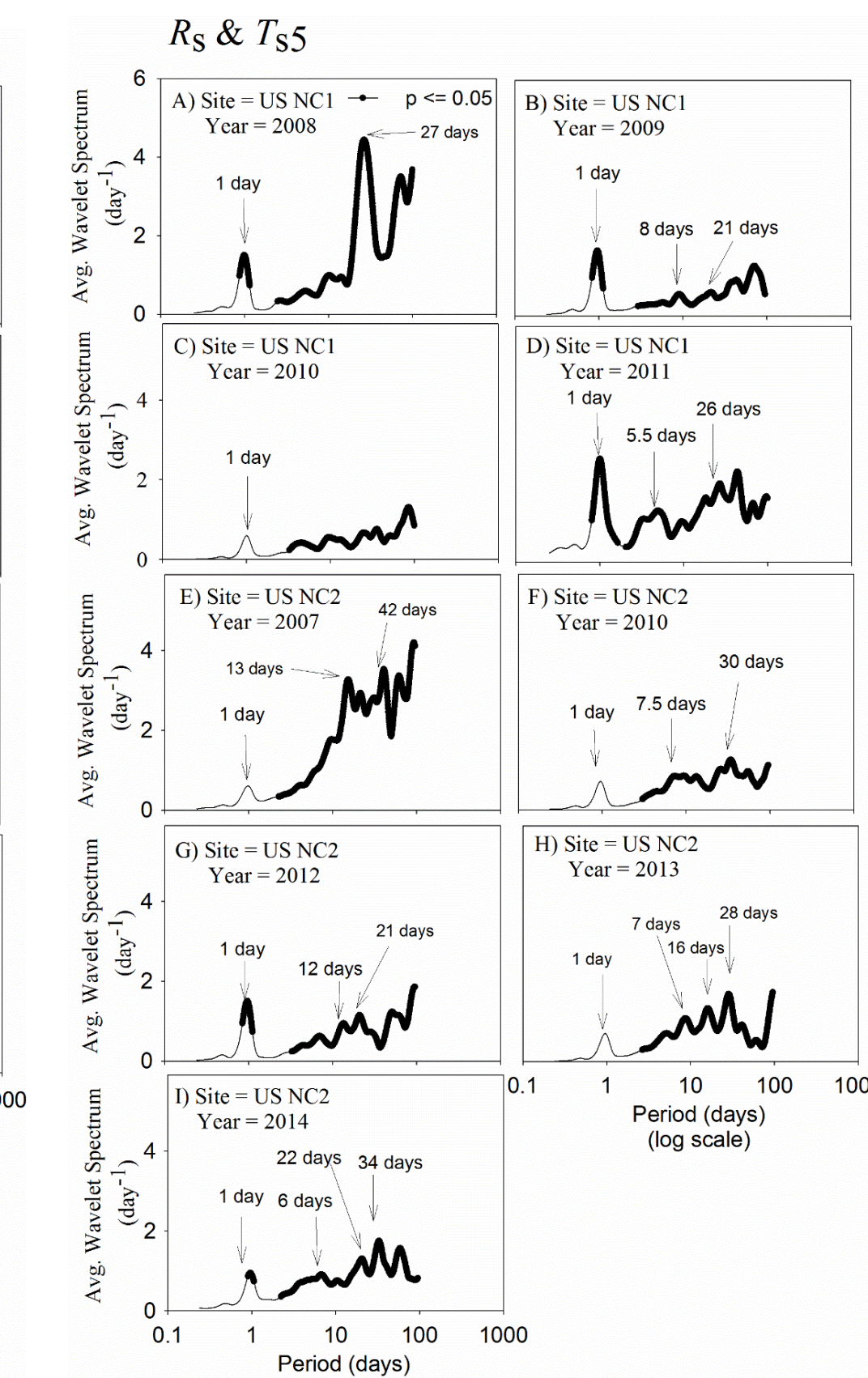


Figure 7: Average wavelet power in the frequency domain generated from CWT transformation of  $R_s$  and  $T_{s5}$  at different sites. The 5% significance level was generated against white noise.

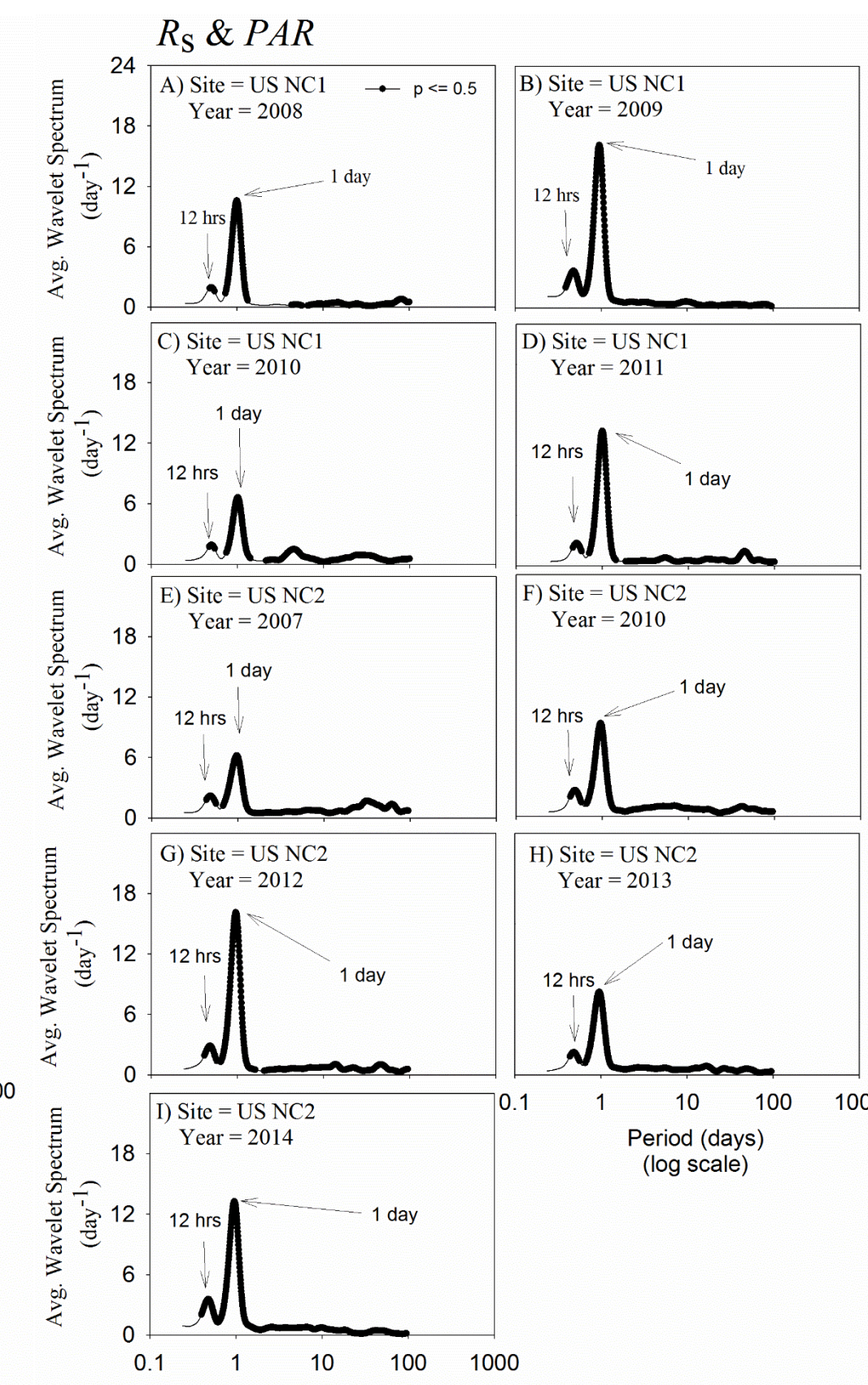


Figure 8: Average wavelet power in the frequency domain generated from CWT transformation of  $R_s$  and PAR at different sites. The 5% significance level was generated against white noise.

## Heat Maps:

Image plot of the cross-wavelet power spectrum in the time-period domain.

The image identifies significant (red color zones) cospectral signatures, with arrows indicating the leading or lagging effects by the drivers

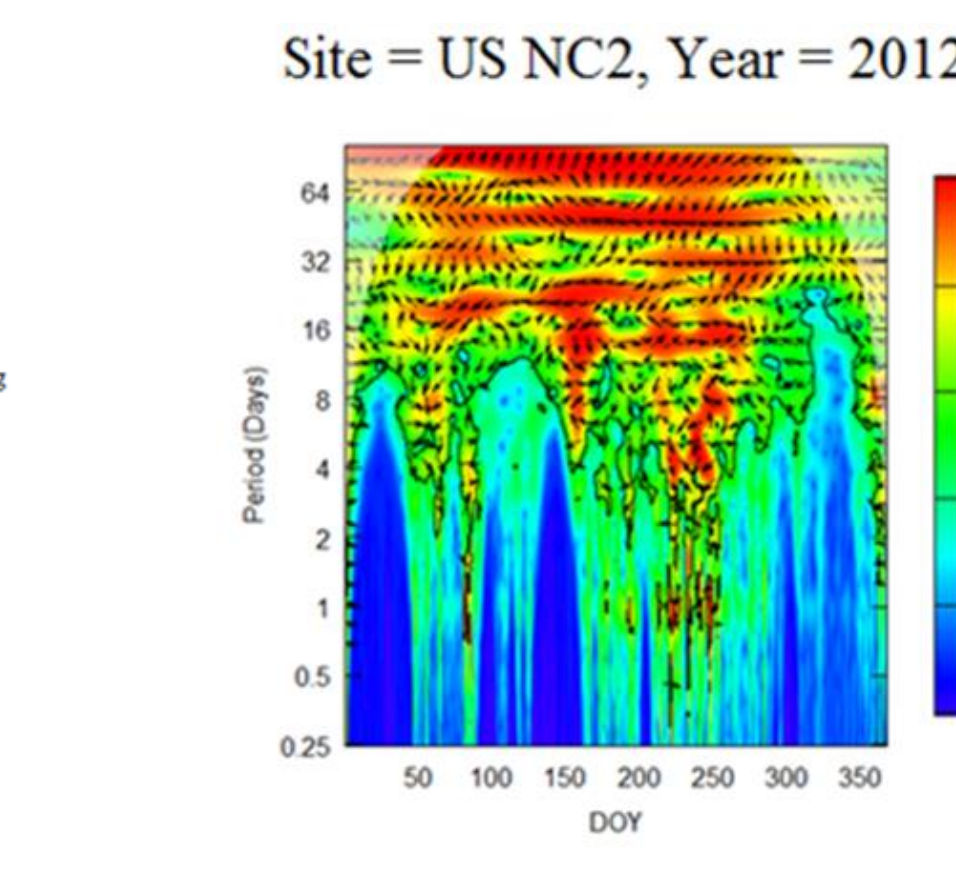
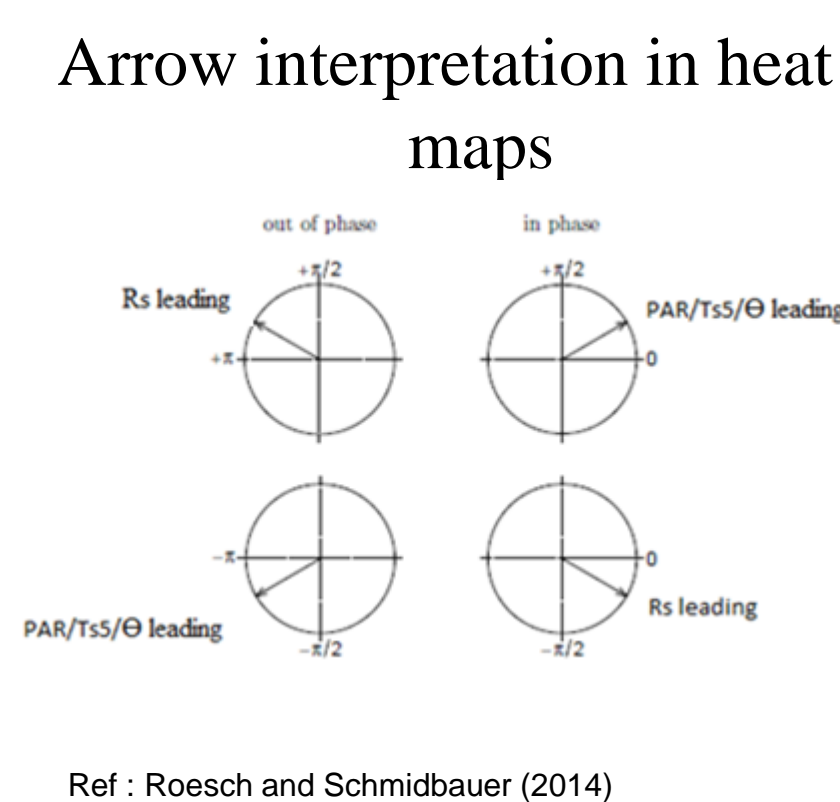


Figure 9: Heat map of CWT analysis between  $R_s$  &  $\theta$

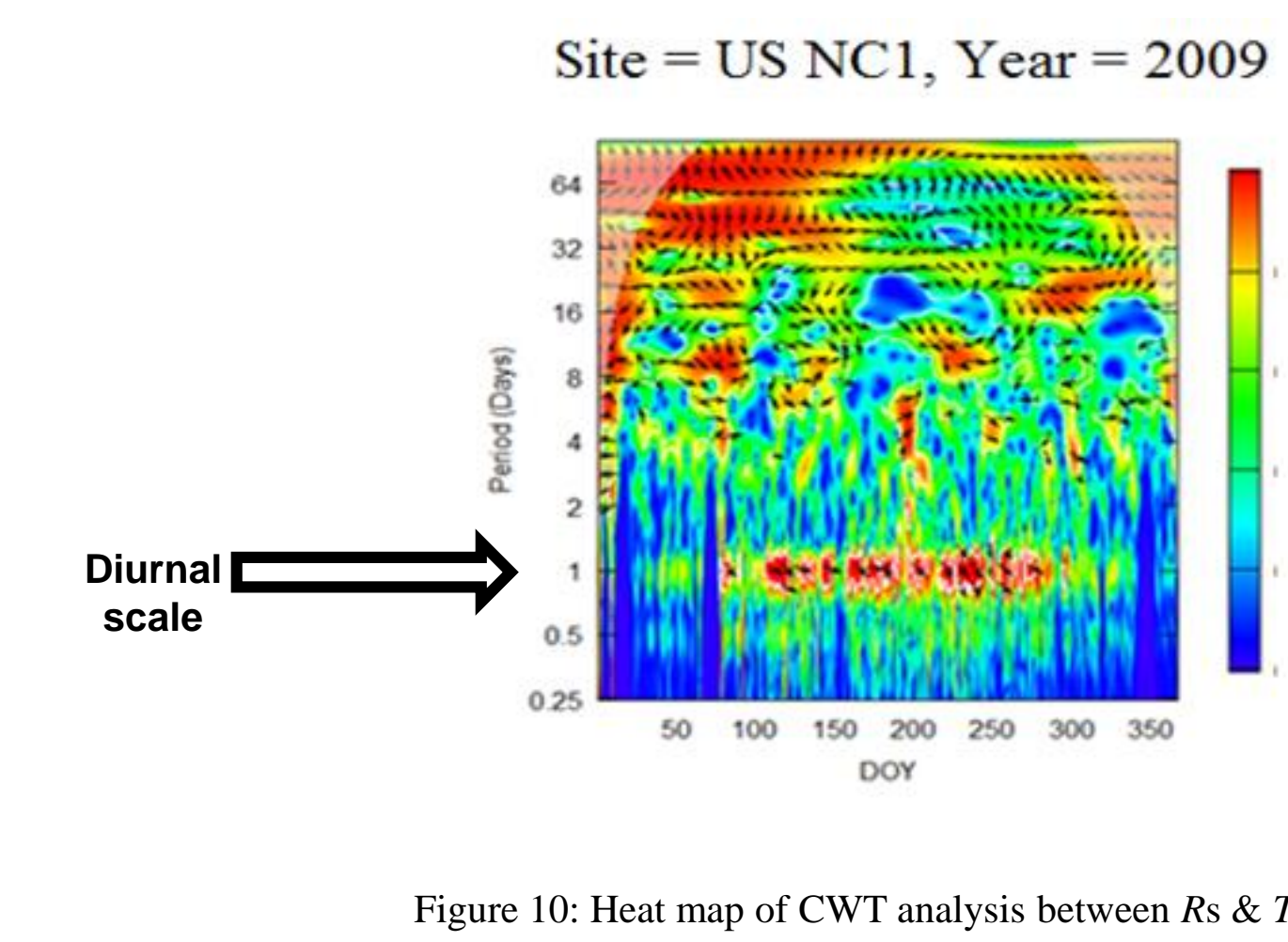


Figure 10: Heat map of CWT analysis between  $R_s$  &  $T_{s5}$

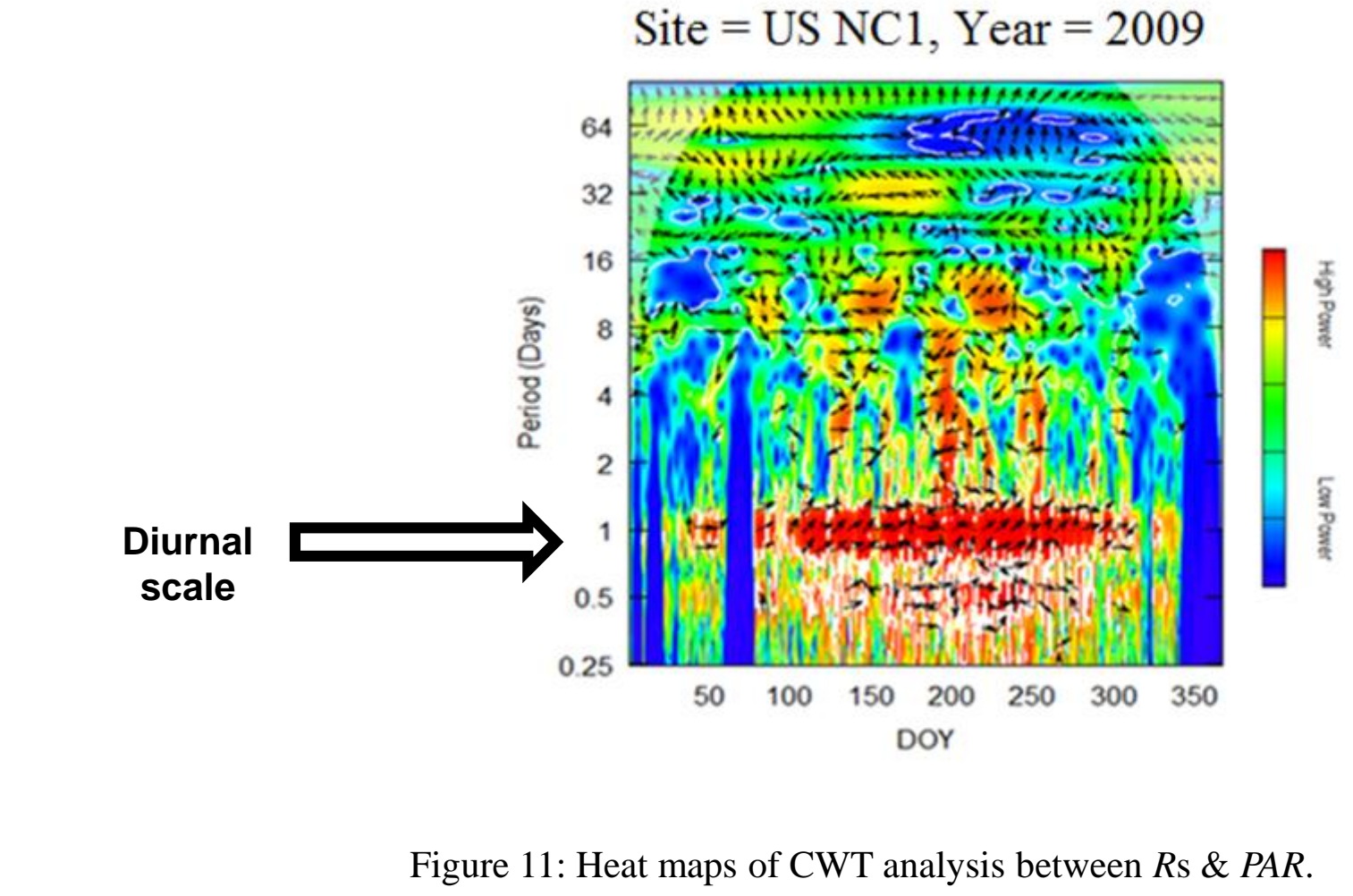


Figure 11: Heat maps of CWT analysis between  $R_s$  & PAR.

## Heat Map Summary (Based on arrow direction):

As we found same trends across all years and at both sites, only certain years have been highlighted.

- Figure 9: No evidence of any consistent phase relationship between  $R_s$  &  $\theta$ .
- Figure 10: At diurnal scale,  $R_s$  leads  $T_{s5}$  during certain days. This suggest hysteresis or presence of temperature-independent component of  $R_s$ .
- Figure 11: At diurnal scale,  $R_s$  lagged PAR during the growing season (DOY 100 – 300).

## Phase Angle to Lag Hours at diurnal scale:

- The phase angle between photosynthesis and  $R_s$  was converted to lag hours (Figure 12).
- The negative lag hour was in 2007 (a dry year). This suggests heterotrophic respiration may have been the dominant carbon flux during that year.
- Overall, lag time was invariant by canopy height. This suggests that carbohydrate transport from canopy to roots was insensitive of phloem length
- This, in turn, lends support to the pressure-concentration wave hypothesis of phloem loading and contradicts with the direct molecular transport theory (Davidson and Holbrook 2009).

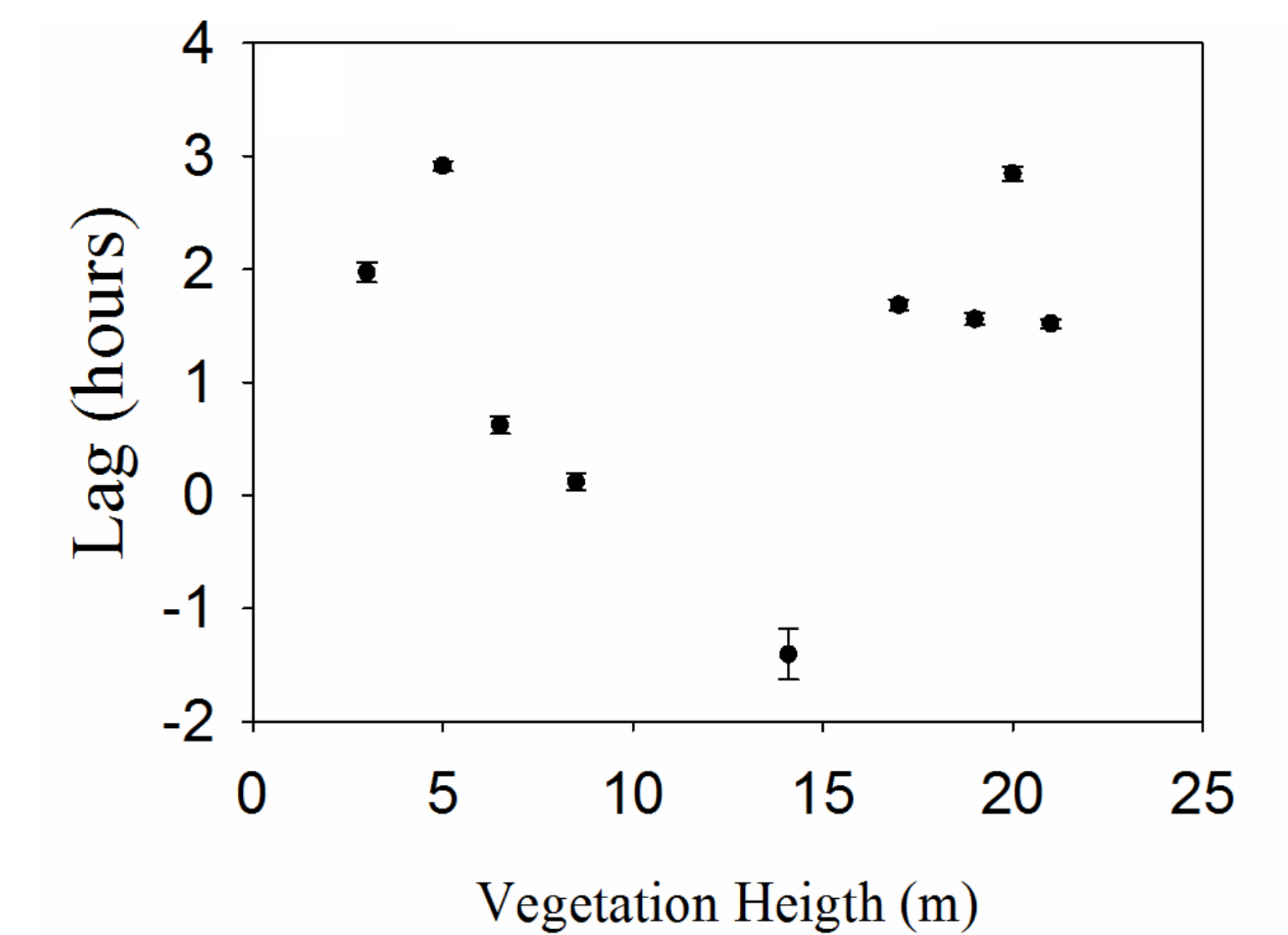


Figure 12: Variation in average lag hours between PAR and  $R_s$  as a function of vegetation height

## Summary

1.  $\theta$ ,  $T_{s5}$  and PAR showed distinct peaks in their cospectra with  $R_s$  (Figure 13).

2. PAR cospectrum had the universal and by far the largest peak at daily frequency, soil temperature covaried on diurnal and synoptic scales, and soil moisture covaried on synoptic and seasonal scales.

3. The different drivers have certain overlapping as well as patent time periods during which they regulate the soil CO<sub>2</sub> efflux (Fig. 13).

4. The covariance between PAR and  $R_s$  was highest when  $R_s$  lagged behind PAR by 1-3 hours.

5. Given the differential coupling of root-dependent and root-independent respiration to substrate availability, this approach offers promise to further separate these components of  $R_s$ .

## Disentangling the different drivers of $R_s$

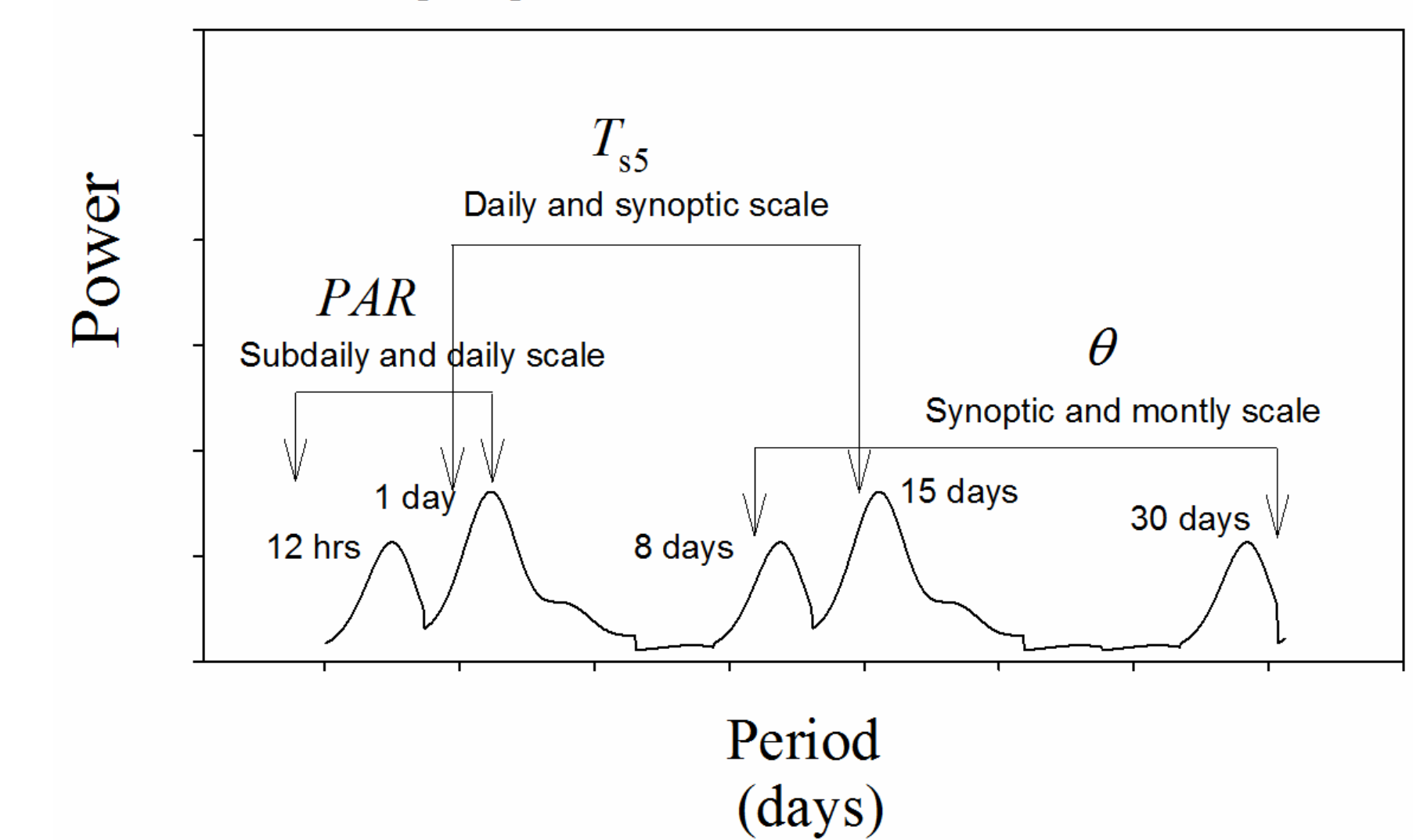


Figure 13: Summary of the CWT analysis between  $R_s$  and biotic and abiotic drivers

- References:
1. Anzi Roesch and Harald Schmidbauer (2014). WaveletComp: Computational Wavelet Analysis. R package version 1.0
  2. Davidson E. A., & Holbrook N. M. (2009). Is temporal variation of soil respiration linked to the phenology of photosynthesis? In A. Noormets, editor. (Ed.), Phenology of ecosystem processes (pp. 187–199). New York, NY, USA: Springer.
  3. Dietze et al. (2011). Characterizing the performance of ecosystem models across time scales: A spectral analysis of the North American Carbon Program site-level synthesis. "Journal of Geophysical Research-Biogeosciences 116.
  4. Stoy et al. (2005). "Variability in net ecosystem exchange from hourly to inter-annual time scales at adjacent pine and hardwood forests: a wavelet analysis." "Tree Physiology 25(7): 887-902.
  5. Stoy et al. (2013). "Evaluating the agreement between measurements and models of net ecosystem exchange at different times and timescales using wavelet coherence: an example using data from the North American Carbon Program Site-Level Interim Synthesis." "Biogeosciences 10(11): 6893-6909.